Tetrahedron 69 (2013) 11130–11137

Contents lists available at ScienceDirect

Tetrahedron

journal homepage: www.elsevier.com/locate/tet

Synthesis of novel chiral bis-*N*-substituted-hydrazinecarboxamide receptors and probing their solution-phase recognition to chiral carboxylic guests by ESI-TOF/MS and tandem ESI-MS

Hany F. Nour [a], Agnieszka Golon [b], Tuhidul Islam [b], Marcelo Fernández-Lahore [b], Nikolai Kuhnert [b,*]

[a] National Research Centre, Department of Photochemistry, El Behoose Street, PO Box 12622, Cairo, Dokki, Egypt
[b] School of Engineering and Science, Centre for Nano and Functional Materials (NanoFun), Jacobs University, 28759 Bremen, Germany

ARTICLE INFO

Article history:
Received 26 May 2013
Received in revised form 21 October 2013
Accepted 4 November 2013
Available online 8 November 2013

Keywords:
Hydrazinecarboxamide
Self-assembly
ESI mass spectrometry
Dicarbohydrazide
Isocyanate

ABSTRACT

Seven novel bis-*N*-substituted-hydrazinecarboxamide receptors were synthesized in good to excellent yields by reacting chiral dicarbohydrazides, obtained from commercially available tartaric acid, with substituted aromatic isocyanates. The newly synthesized hydrazinecarboxamides formed structurally unique supramolecular aggregates, which have been confirmed by ESI-TOF/MS and tandem ESI-MS. They also showed molecular recognition to a selection of chiral carboxylic guests and oligopeptides, which mimic the backbone structure of the bacterial cell wall. The structures of the novel compounds were verified by various spectroscopic techniques including FTIR, ^{1}H NMR, ^{13}C NMR, ESI-TOF/MS, tandem ESI-MS, 2D ROESY NMR, and CD spectroscopy.

1. Introduction

Over the past decades, molecular self-assembly (MSA) has emerged as a stupendous field of endeavors in supramolecular chemistry.[1] MSA has a wide range of applications in biology, nanochemistry, and material science.[2] In order for molecules to undergo self-organization, they must possess functionalities, which aid formation of complementary structures.[3] Noncovalent interactions, such as hydrogen bonds and π–π-stacking play a prominent role in holding and thus stabilizing the assembled associations.[4] In most cases, the self-assembled structures can possess attractive and distinct properties, which differ entirely from that of the non-assembled precursors.[5] An example from nature, which demonstrates the concept of MSA is the self-assembly of the tobacco mosaic virus (TMV).[6] The helical structure of TMV forms by self-assembly of a defined number of protein subunits around a single strand of ribonucleic acid (RNA). Another common example is the Watson–Crick base pairing model in deoxyribonucleic acid (DNA), in which the building blocks assemble together to form a precise and extremely well ordered double helix strand of encoded genetic information. Peptide amphiphiles (PAs), which were firstly reported by Stupp and co-workers, spontaneously formed high molecular weight cylindrically nanofibers.[7] Both the hydrophobicity and hydrogen bonds participate cooperatively in the formation of the self-assembled aggregates.[7]

Mass spectrometry (MS) has been extensively used in studying noncovalent interactions.[8] The detection of biological macromolecules, host/guest (H/G) complexes or self-assembled associations became possible with the development of soft-ionization MS techniques, such as electrospray ionization (ESI). An important feature of ESI-MS is that the solution-phase information can be retained into the gas phase. However, there are some limitations and obstacles associated with detecting high ordered self-assembled structures. These obstacles usually include low peak intensities of the complexes or decomposition of the intact assembled associations before reaching the detector.

Recently, we reported on the synthesis of a new class of chiral cyclophane-*type* macrocycles (**A**) and (**B**) in almost quantitative yields (Fig. 1).[9] We showed that the macrocycles could be obtained in both enantiomeric forms (*R*) or (*S*) by reacting chiral dicarbohydrazides, obtained from commercially available diethyl tartrate, with aromatic dialdehydes and diisocyanates in [2+2]

* Corresponding author. Tel.: +49 421 200 3120; fax: +49 421 200 3229; e-mail addresses: hany.nour@daad-alumni.de (H.F. Nour), n.kuhnert@jacobs-university.de (N. Kuhnert).

0040-4020/$ – see front matter © 2013 Elsevier Ltd. All rights reserved.
http://dx.doi.org/10.1016/j.tet.2013.11.002

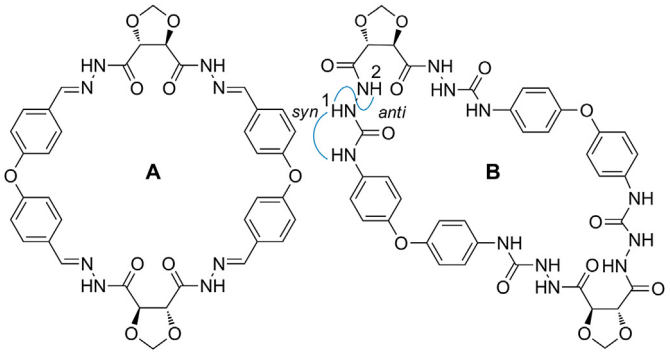

Fig. 1. Tetra-(carbohydrazide) cyclophane (**A**) and tetra-(hydrazinecarboxamide) cyclophane (**B**).

macrocyclization reactions. In this contribution, we report on the synthesis of new bis-*N*-substituted-hydrazinecarboxamides with hydrazido urea functionalities and assessment of their solution-phase recognition to a selection of chiral carboxylic guests by using electrospray ionization time-of-flight mass spectrometry (ESI-TOF/MS) and tandem ESI-MS. Parallel to our work with cyclophanes (**A**) and (**B**), Gawroński and co-workers reported on the synthesis of a tetra-(carbohydrazide) cyclophane macrocycle from (4*R*,5*R*)-2,2-dimethyl-1,3-dioxolane-4,5-dicarbohydrazide and terephthaldehyde.[10] Macrocycle (**A**) possesses four acylhydrazone moieties, making it suitable for different applications in dynamic combinatorial chemistry (DCC), while macrocycle (**B**) possesses more functionalities and has a higher degree of flexibility.[9,11] Similar to the case of trianglimine chemistry, macrocycles (**A**) and (**B**) were formed under the conformational bias of the dicarbohydrazide precursor.[12]

2. Results and discussion

2.1. Synthesis and conformational analysis

In continuation to our work with cyclophane macrocycles (**A**) and (**B**), we report on the synthesis of a new class of two-armed receptors (**7**–**13**), which mimic the backbone structure of macrocycle (**B**). The receptors of this kind were expected to show a high degree of flexibility. The new receptors (**7**–**13**) were obtained from the reactions of chiral dicarbohydrazides (**1**–**3**) with substituted aromatic isocyanate (**4**–**6**) in anhydrous THF (Fig. 2). The structures of compounds (**7**–**13**) were verified by various spectroscopic techniques including FTIR, ^{1}H NMR, ^{13}C NMR, 2D ROESY, circular dichroism (CD) spectroscopy, ESI-TOF/MS, and tandem MS. The ^{1}H NMR spectrum of (**7**) showed three broad signals at δ 10.05, 8.54, and 8.04 ppm corresponding to the six amidic N*H* protons.

The FTIR spectrum showed a strong absorption band at ν 1689 cm^{-1}, corresponding to the stretching vibration of the C=O moieties. The ESI-TOF/MS, in the negative ion mode, showed the expected molecular ion peak at *m*/*z* 487.1588 as [M−H]$^-$. The high resolution mass spectrometry (HRMS) data for the new receptors are shown in Table 1.

The 2D ROESY spectrum of receptor (**7**) (Fig. 3) showed through space interactions between H^c–H^d and H^d–H^e, which suggested a *syn*/*syn* conformation of the N*H* moieties. Unlike in the case of receptor (**7**), the N*H* moieties in macrocycle (**B**) assume a *syn*/*anti* conformation.[9c] It is worth noting that the *syn*/*syn* conformer of macrocycle (**B**) has more energy than the *syn*/*anti* or the *anti*/*anti* conformers due to the electrostatic repulsion between the C=O moieties (6)-(9), (21)-(24), (27)-(30), and (3)-(42).[9c] In order to further understand the reasons for the preferential formation of the

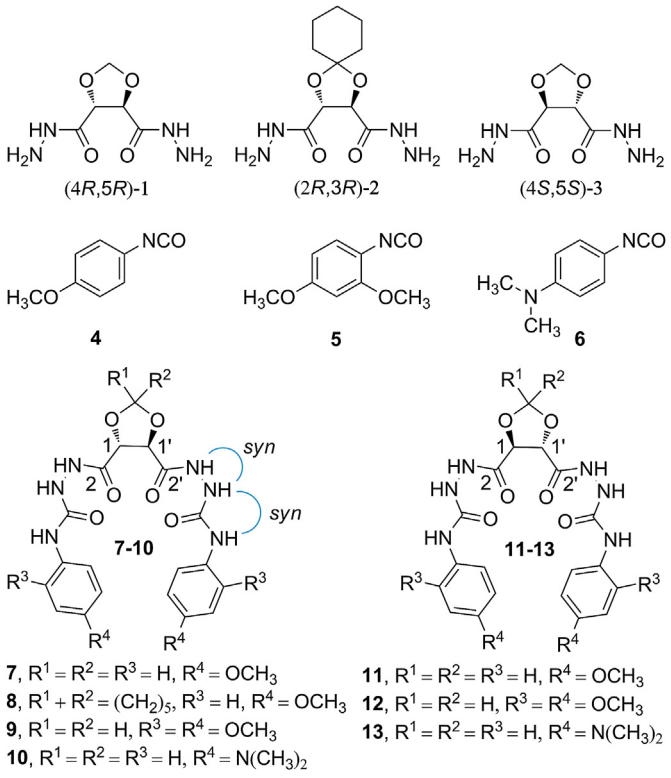

Fig. 2. Two-armed receptors (**7**–**13**) obtained through addition of chiral dicarbohydrazides (**1**–**3**) to substituted aromatic isocyanates (**4**–**6**) in THF.

Table 1
ESI-TOF/MS data and yields of receptors (**7**–**13**)

Product	Molecular formula	Calcd *m*/*z*	[a]Found *m*/*z*	Error [ppm]	Yield %
7	$C_{21}H_{24}N_6O_8$	487.1583	487.1588	−1.0	78
8	$C_{26}H_{32}N_6O_8$	555.2209	555.2224	−2.8	74
9	$C_{23}H_{28}N_6O_{10}$	547.1794	547.1782	2.2	93
10	$C_{23}H_{30}N_8O_6$	513.2216	513.2240	−4.8	89
11	$C_{21}H_{24}N_6O_8$	487.1583	487.1570	2.7	96
12	$C_{23}H_{28}N_6O_{10}$	547.1794	547.1799	−1.0	99
13	$C_{23}H_{30}N_8O_6$	513.2216	513.2233	−3.5	93

[a] Products detected as [M−H]$^-$ ions.

syn/*syn* conformer over the *syn*/*anti* or the *anti*/*anti* conformers for receptor (**7**), we performed molecular modeling studies at the Austin Model 1 (AM1) level using HyperChem software (Release 8.0.6).[13] Data from the 2D ROESY NMR were used for subsequent structure modeling calculations. Molecular modeling suggested a spiral-*like* structure for (**7**), in which the N*H* moieties are *syn*/*syn* oriented with possibility of formation of two intramolecular hydrogen bonds between (N*H*···O=C) (3)-(5′) and (3′)-(5). These interactions stabilize the structure of (**7**) and reduce the electrostatic repulsion between the C=O moieties (2)-(5) and (2′)-(5′) (Fig. 4).

2.2. Probing solution-phase recognition of receptors (7–13) to chiral carboxylic guests (14–20) by using ESI-TOF/MS

ESI-MS has been widely used as a versatile soft ionization method in studying weak noncovalent interactions.[8,14] The ability of the technique to provide precise mass values, high resolution, and little or almost no fragmentations, makes it an indispensable tool in supramolecular analysis. Recently, we reported on the use of ESI-TOF/MS in probing the mechanism of trianglimine formation in real-time and studying the dynamic reversibility and molecular recognition of the tetra-(carbohydrazide) cyclophane macrocycles

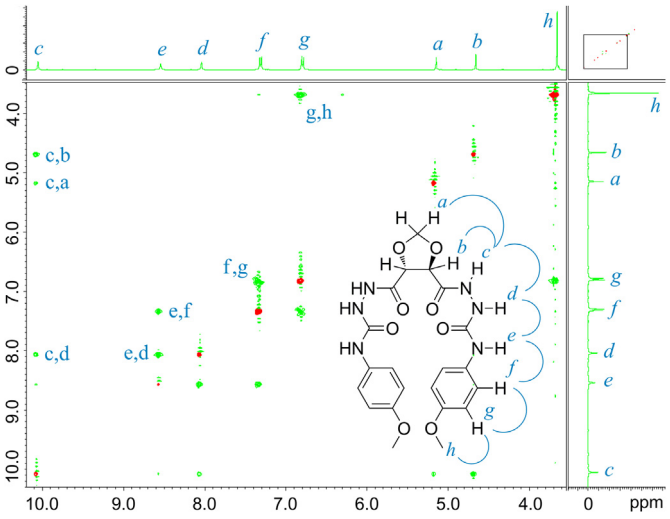

Fig. 3. 2D ROESY NMR spectrum of receptor (**7**) (DMSO-d_6).

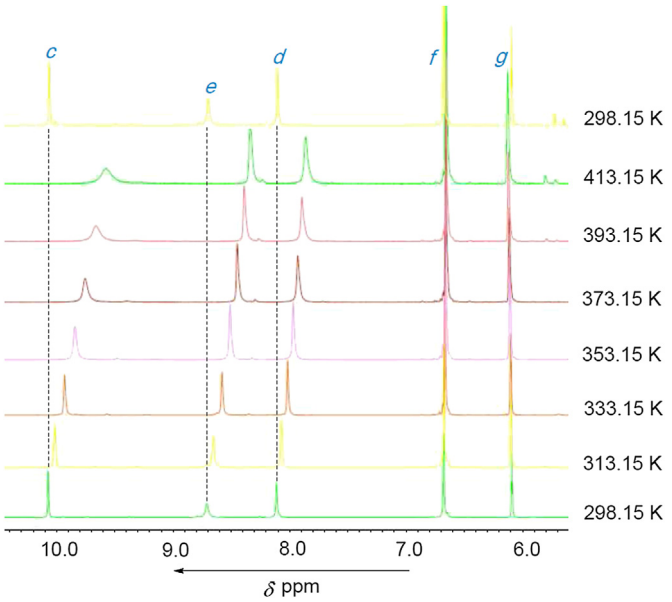

Fig. 5. Stacked VT NMR spectra of receptor (**7**) (400 MHz, DMSO-d_6, 298.15–413.15 K).

to oligopeptides.[11,15] The novel receptors (i.e., **7**) formed interesting self-assembled dimeric, trimeric, and tetrameric supramolecular associations.

The behavior of the new receptors toward increasing temperature was investigated by performing variable temperature NMR (VT NMR) studies. The VT NMR experiment for receptor (**7**) was performed from 313.15 to 413.15 K in DMSO-d_6 (Fig. 5). By increasing temperature, the N*H* moieties of receptor (**7**) showed significant downfield chemical shifts. The decrease in δ (ppm) for NH^c, NH^e, and NH^d is a consequence of breaking inter- or intramolecular hydrogen bonds (N*H*···O═C). Cooling the NMR to 298.15 K gave the same spectrum as first recorded due to the re-establishment of the hydrogen bonds. The molecular self-assembly of (**7**) was investigated by ESI-TOF/MS and MS/MS. The tandem ESI mass spectra for the self-assembled associations of (**7**) are shown in Fig. 6(b–d).

The ESI-TOF/MS of (**7**) (Fig. 6a) showed four peaks at *m*/*z* 511.2, 999.4, 1487.6, and 1976.8, corresponding to the sodiated molecular ion peaks of the free receptor, dimeric, trimeric, and tetrameric self-assembled structures, respectively.

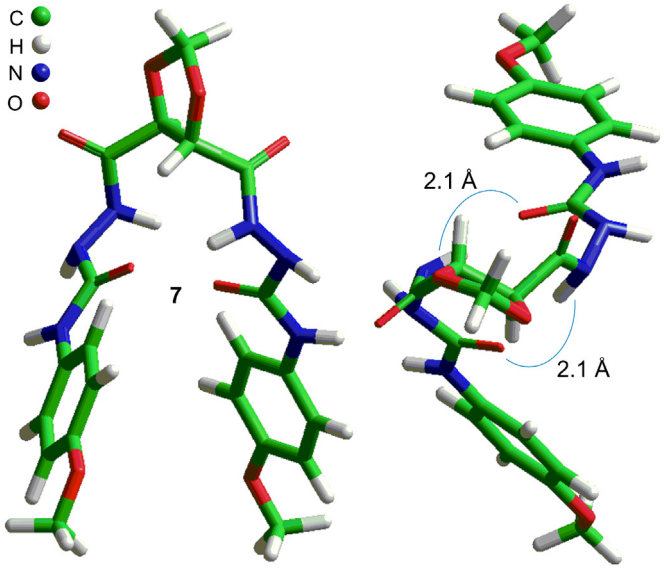

Fig. 4. Computed structure of receptor (**7**) at the AM1 level. A Polak–Ribiere conjugate gradient with rms 0.01 kcal mol^{-1} was used.

Molecular modeling at the semi-empirical parameterized model **3** (PM3) level for two assembled molecules of (**7**) suggested that the receptor molecules were lined up in a queue-*like* structure and connected together by two intermolecular hydrogen bonds forming between (N*H*···O═C) (4)-(5) and (4′)-(5′) (Fig. 7, A). Further probable structures (B–E) were not taken into consideration because they could not permit formation of intermolecular hydrogen bonds.

Proposed fragmentation mechanisms of the self-assembled associations of receptor (**7**) are shown in Fig. 8. Interestingly, the novel receptors (i.e., **7**) showed unprecedented recognition to the carboxylic guests and oligopeptides (**14**–**20**) with formation of 1:1, 1:2, 1:3, and 2:1 complexes, which have been confirmed by ESI-TOF/MS and MS/MS (Scheme 1 and Table 2). Up to six assembled associations of receptor (**7**) were observed and unambiguously assigned by ESI-TOF/MS and tandem ESI-MS (see the Supplementary data). The tandem ESI-MS of the supramolecular complex (**7**/**14**) showed a peak at *m*/*z* 1168.3, corresponding to two assembled molecules of (**7**) with a one molecule of D-(−)-quinic acid (**14**) (Fig. 9c). It gave upon fragmentation three peaks appearing at *m*/*z* 487.0, 679.1, and 975.2 (base peak), which confirmed self-assembly in the order shown in Fig. 10a (structure S1). Structure (S2) was excluded because its fragmentation could not yield a peak at *m*/*z* 975 for the intermolecular bonded two molecules of (**7**).

Another interesting example is the self-assembly of the supramolecular complex (**7**/**16**) (for HRMS and MS/MS spectra, see the Supplementary data). The tandem ESI mass spectrum of the H/G complex (**7**/**16**) showed a peak at *m*/*z* 1613 for three assembled molecules of (**7**) with a one molecule of L-(+)-tartaric acid (**16**). The MS/MS of this complex gave five intense peaks appearing at *m*/*z* 1463.3, 1125.2, 975.2 (base peak), 636.9, and 486.9. These fragments were assigned to three self-assembled molecules of (**7**), two molecules of (**7**) with a one molecule of (**16**), two molecules of (**7**), a one molecule of (**7**) with a one molecule of (**16**), and the free receptor (**7**), respectively. It can be clearly understood that three molecules of (**7**) were directly linked by intermolecular hydrogen bonds and the guest, L-(+)-tartaric acid (**16**), bound to the first member in the assembly. The ESI-TOF/MS and MS/MS for the self-assembled aggregates (**7**/**14**–**20**) are shown in Supplementary data.

In solution, we investigated the effect of increasing the molar equivalency of D-(−)-quinic acid (**14**), in a mixture of (**7**/**14**), on the δ (ppm) of the N*H* and O*H* protons. A small upfield shift

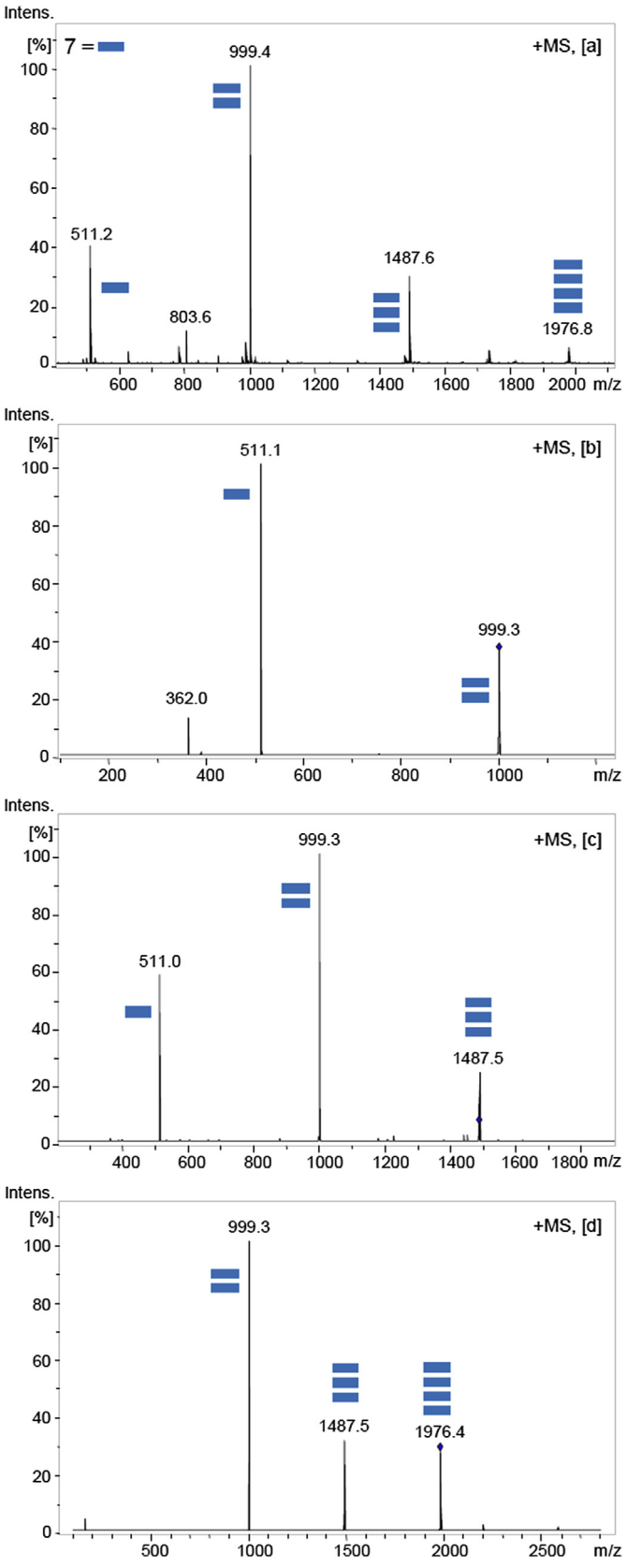

Fig. 6. Self-assembled associations of receptor (**7**) in the positive ion mode, (a) ESI-TOF/MS, (b–d) tandem ESI-MS of the self-assembled associations. Products detected as $[M+Na]^+$ ions.

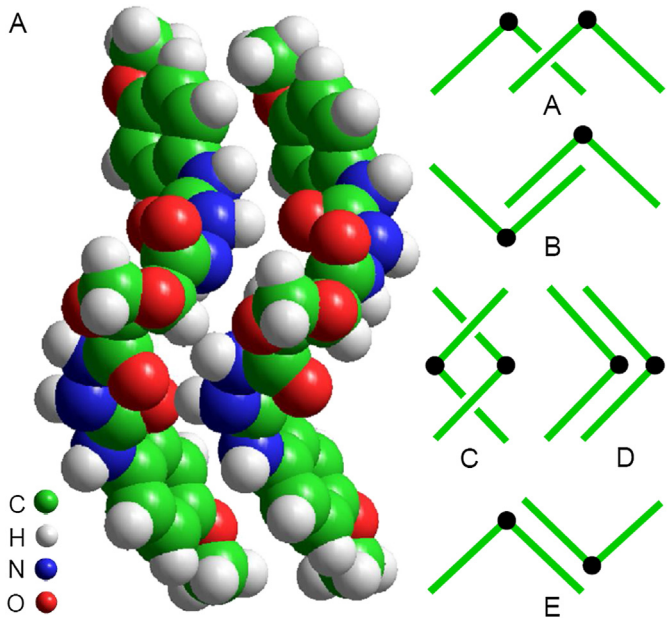

Fig. 7. Bird's-eye view for a proposed computed structure of two assembled molecules of (**7**). Structures were energy minimized at the PM3 level. A Polak–Ribiere conjugate gradient with rms 0.01 kcal mol^{-1} was used.

(−0.0012 ppm) was observed for the three hydroxyl groups (O*H*^{3}, O*H*^{4}, and O*H*^{5}), while (O*H*^{1}) showed a small downfield shift (+0.008 ppm) at a stoichiometry of 1:10 of (**7**/**14**). The N*H* protons of (**7**) showed upfield shifts of (−0.0252 ppm), (−0.0149 ppm), and (−0.0069 ppm) for N*H*^{c}, N*H*^{e}, and N*H*^{d}, respectively. The (Ar*H*) showed upfield shifts of (−0.0131 ppm) and (−0.008 ppm) for Ar*H*^{f} and Ar*H*^{g}, respectively. It can be inferred that the carboxylic proton (COO*H*) of (**14**) formed an intermolecular hydrogen bond with either C=O (2) or (5) of receptor (**7**), while the N*H* protons did not participate directly in these interactions (for stacked ^{1}H NMR spectra of complex (**7**/**14**), see the Supplementary data). We performed a 2D ROESY NMR experiment to investigate the exact binding mode in complex (**7**/**14**).

Unfortunately no through space interactions were observed between host (**7**) and guest (**14**) due to the long through space distance between the protons. The slightly small shift of the N*H* signals of (**7**) in response to addition of (**14**) could be a consequence of the competitive recognition of the H/H and H/G assembles in

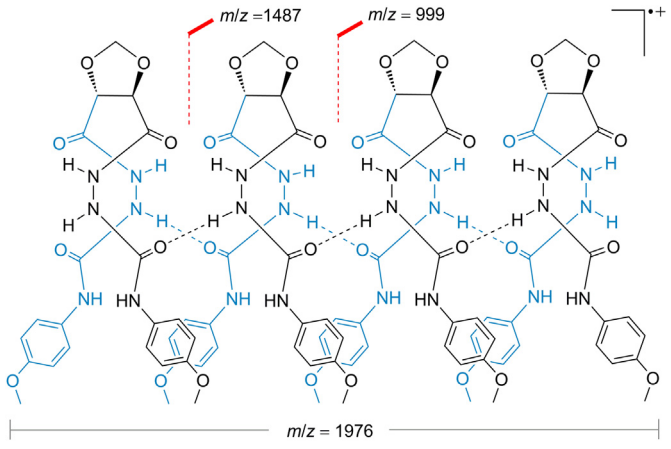

Fig. 8. Proposed structure and fragmentation mechanism for self-assembled four molecules of receptor (**7**).

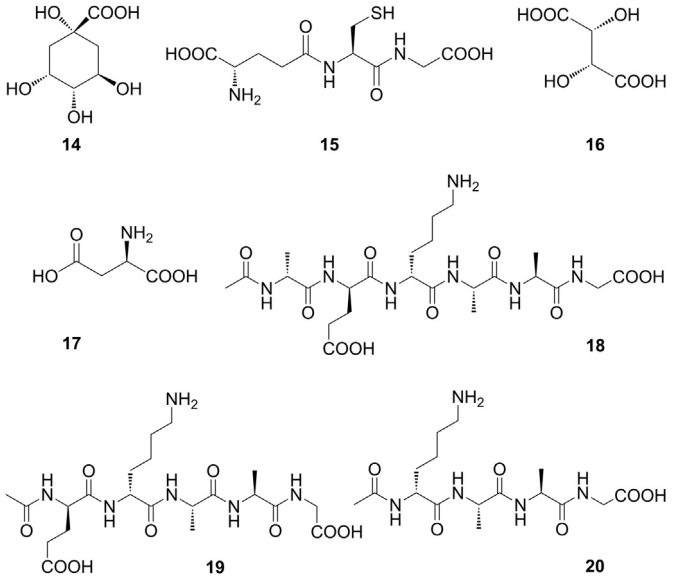

Scheme 1. A selection of chiral carboxylic guests and oligopeptides (**14**–**20**).

solution. It also could be attributed to the competing effect of the solvent.

2.3. Recognition of receptors (7), (9), and (10) to oligopeptides (18–20)

The molecular recognition of the new receptors to the chiral carboxylic guests has inspired us to assess the interactions of a mixture of different hosts with the oligopeptide guests (**18**–**20**). The recognition of receptors (**7**), (**9**), and (**10**) to oligopeptides (**18**–**20**), which mimic the backbone structure of the bacterial cell wall, was investigated by ESI-TOF/MS and tandem ESI-MS. Three experiments were conducted for equimolar mixtures of receptors (**7**, **9**), (**7**, **10**), and (**7**, **9**, and **10**) with oligopeptides (**18**–**20**) (Table 3 and Fig. 11a–c). Supramolecular complexes with mass peaks of 1:1, 1:2, and 2:1 stoichiometries were observed.

The ESI-TOF/MS for a mixture of (**7**), (**9**), and (**18**) showed H/G peaks appearing at *m*/*z* 1076.4 and 1136.4 for complexes (**7**/**18**) and (**9**/**18**), respectively (Fig. 11a). Two H/G mass peaks appeared at *m*/*z* 1076.4 and 1102.5 in a mixture of (**7**), (**10**), and (**18**) (Fig. 11b). In the last experiment equimolar quantities of receptors (**7**), (**9**), and (**10**) were mixed with guest (**18**). Three H/G complex peaks were observed at *m*/*z* 1076.4, 1102.5, and 1136.4, corresponding to complexes (**7**/**18**), (**10**/**18**), and (**9**/**18**), respectively (Fig. 11c). The peak intensities of the complexes don't reflect the actual distribution of the complexes in solution or correlate with their stabilities, since the ionization efficiency in ESI-MS is still dependent on the desolvation energies of the individual complexes. Interestingly, we observed mass peaks for stable H/G complexes of two different receptors binding with a one molecule of the oligopeptide guests. The ESI-TOF/MS for a mixture of (**7**), (**9**), and (**19**) showed a peak at *m*/*z* 1553.6, corresponding to the supramolecular complex (**7**/**9**/**19**). It gave upon dissociation two peaks at *m*/*z* 1003.2 (**7**/**19**) and 515.1

Table 2
ESI-TOF/MS data of the H/G complexes (**7**/**14**–**20**)

Complex	Molecular Formula	Calcd *m*/*z*	Meas. *m*/*z*	Error [ppm]
$\mathbf{7}^{H}/\mathbf{14}^{a,G}$	$C_{28}H_{36}N_6O_{14}$	679.2217	679.2248	−4.6
$\mathbf{7}^{H}/\mathbf{14}^{b,G}$	$C_{49}H_{60}N_{12}O_{22}$	1167.3872	1167.3888	−1.3
$\mathbf{7}^{H}/\mathbf{14}^{c,G}$	$C_{70}H_{84}N_{18}O_{30}$	1655.5528	1655.5529	−0.1
$\mathbf{7}^{H}/\mathbf{15}^{d,G}$	$C_{31}H_{41}N_9O_{14}S$	796.2566	796.2573	−0.8
$\mathbf{7}^{H}/\mathbf{15}^{e,G}$	$C_{52}H_{65}N_{15}O_{22}S$	1284.4222	1284.4226	−0.3
$\mathbf{7}^{H}/\mathbf{16}^{a,G}$	$C_{25}H_{30}N_6O_{14}$	637.1747	637.1777	−4.6
$\mathbf{7}^{H}/\mathbf{16}^{b,G}$	$C_{46}H_{54}N_{12}O_{22}$	1125.3403	1125.3447	−3.9
$\mathbf{7}^{H}/\mathbf{16}^{c,G}$	$C_{67}H_{78}N_{18}O_{30}$	1613.5058	1613.5082	−1.5
$\mathbf{7}^{H}/\mathbf{17}^{a,G}$	$C_{25}H_{31}N_7O_{12}$	620.1958	620.1976	−2.9
$\mathbf{7}^{H}/\mathbf{18}^{d,G}$	$C_{45}H_{65}N_{13}O_{18}$	1076.4643	1076.4673	−2.8
$\mathbf{7}^{H}/\mathbf{19}^{d,G}$	$C_{42}H_{60}N_{12}O_{17}$	1005.4272	1005.4289	−1.7
$\mathbf{7}^{H}/\mathbf{19}^{e,G}$	$C_{63}H_{84}N_{18}O_{25}$	1493.5928	1493.5875	3.6
$\mathbf{7}^{H}/\mathbf{20}^{d,G}$	$C_{37}H_{53}N_{11}O_{14}$	876.3846	876.3864	−2.0
$\mathbf{7}^{H}/\mathbf{20}^{f,G}$	$C_{53}H_{82}N_{16}O_{20}$	1263.5964	1263.5964	0

Products detected as (*a*) $[(M^H+M^G)-H]^-$, (*b*) $[(2M^H+M^G)-H]^-$, (*c*) $[(3M^H+M^G)-H]^-$, (*d*) $[(M^H+M^G)+H]^+$, (*e*) $[(2M^H+M^G)+H]^+$, and (*f*) $[(M^H+2M^G)+H]^+$.

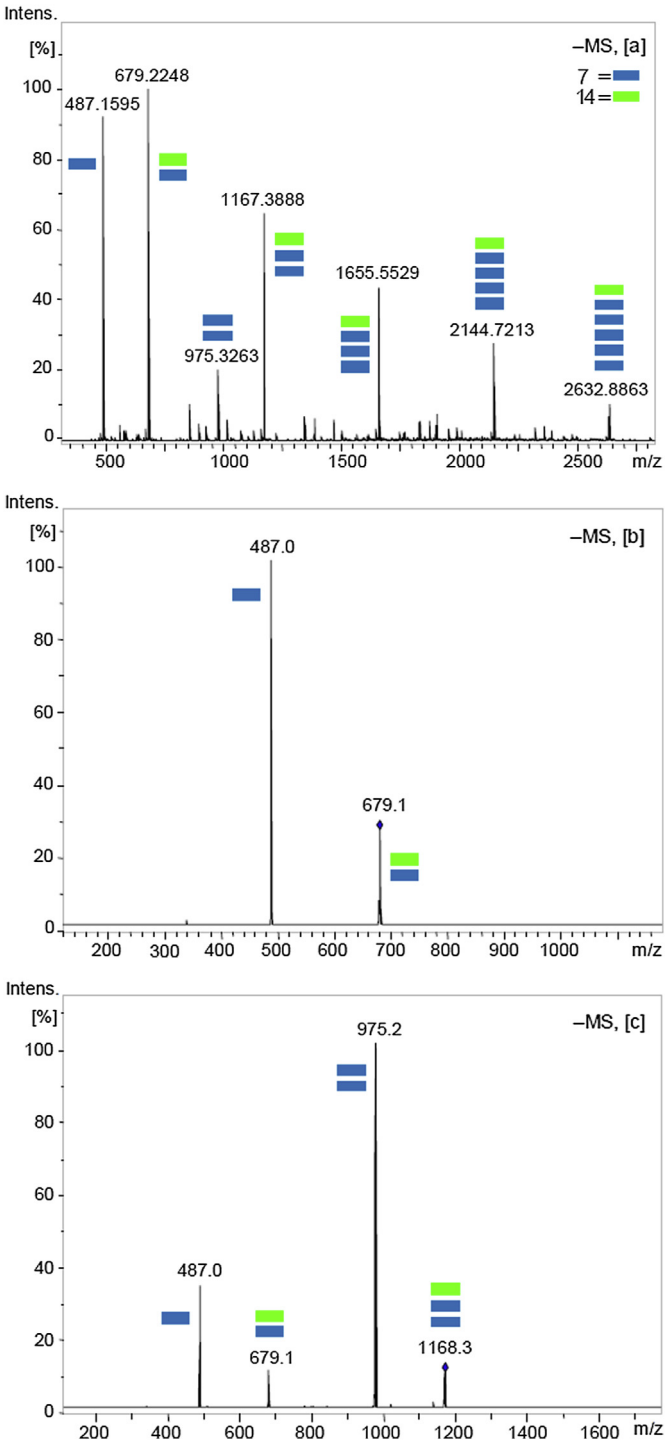

Fig. 9. Self-assembled supramolecular complex (**7**/**14**), (a) ESI-TOF/MS, (b and c) tandem ESI-MS for the assembled associations of (**7**/**14**). Product detected as $[M-H]^-$ ions.

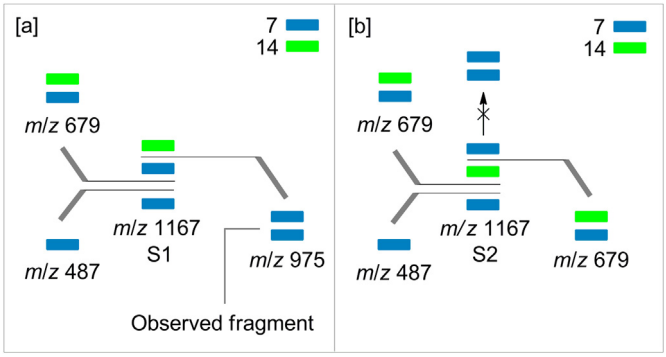

Fig. 10. Proposed assembly and fragmentation mechanism of the supramolecular complex (**7**/**14**).

(**19**). The order of assembly can accordingly be (**9**/**7**/**19**) or (**7**/**19**/**9**). Both structures can dissociate to give the H/G complex (**7**/**19**) (see the Supplementary data). Macrocycle (**B**), which has a similar backbone structure to (**7**), cannot form complex structures in this order.[16] ESI-TOF/MS for higher molecular weight assembles are shown in Supplementary data.

The chirality of the novel compounds (**7**–**13**) was confirmed by CD spectroscopy (Fig. 12). The CD spectrum of receptor (**7**) showed a bisignate Cotton effect with a negative sign at around 250 nm and a positive sign at around 255 nm, which indicated a strong excitation coupling between the chromophores. Also, receptor (**7**) showed larger molar ellipticity in comparison with its stereoisomer (**11**).

3. Conclusion

In summary, a novel class of chiral non-racemic two-armed receptors has been synthesized from the addition reactions of chiral dioxolane dicarbohydrazides to substituted aromatic isocyanates. The receptors adopt a *syn*/*syn* conformation in solution, which is stabilized by intramolecular hydrogen bonds. They exhibited molecular self-assembly and formed unprecedented queue-*like* aggregates with a selection of chiral carboxylic guests and oligopeptides. To the best of our knowledge, assembly in this order has never been reported in the Literature. The formed supramolecular assemblies were stabilized by intermolecular hydrogen bonds. The receptors showed a remarkable degree of flexibility in comparison with macrocycles (**A**) and (**B**). Furthermore, the new dioxolanes can be obtained in good yields as analytically and enantiomerically pure products. We expect applications of these receptors in understanding noncovalent interactions, binding with metal ions or developing new chemical sensors.

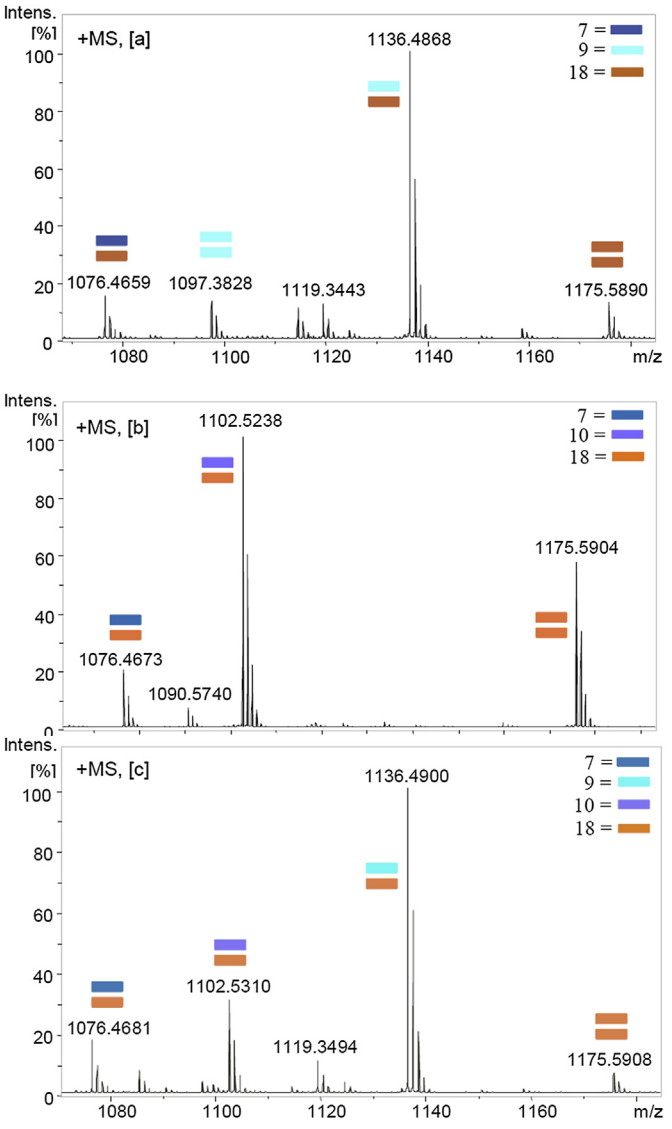

Fig. 11. ESI-TOF/MS for recognition of receptors (**7**), (**9**), and (**10**) to oligopeptide (**18**), (a) (**7**/**9**/**18**), (b) (**7**/**10**/**18**), and (c) (**7**/**9**/**10**/**18**).

4. Experimental section

4.1. General

All the reagents used for the reactions were purchased from Sigma–Aldrich, Applichem or Flucka (Germany), and were used as

Table 3
ESI-TOF/MS data for recognition of receptors (**7**), (**9**), and (**10**) to oligopeptide (**18**)

H/G complex	Molecular Formula	Product ions[a]	Calcd *m*/*z*	Found *m*/*z*	Error [ppm]
(**7** and **9**/**18**)	$C_{45}H_{65}N_{13}O_{18}$	$[(M^{7}+M^{18})+H]^+$	1076.4643	1076.4659	−1.5
	$C_{46}H_{56}N_{12}O_{20}$	$[(2M^{9})+H]^+$	1097.3807	1097.3828	−1.9
	$C_{47}H_{69}N_{13}O_{20}$	$[(M^{9}+M^{18})+H]^+$	1136.4855	1136.4868	−1.2
	$C_{48}H_{82}N_{14}O_{20}$	$[2M^{18}+H]^+$	1175.5903	1175.5890	1.0
	$C_{70}H_{97}N_{19}O_{30}$	$[2M^{9}+M^{18}+H]^+$	1684.6721	1684.6755	−2.0
(**7** and **10**/**18**)	$C_{45}H_{65}N_{13}O_{18}$	$[(M^{7}+M^{18})+H]^+$	1076.4673	1076.4643	−2.7
	$C_{48}H_{82}N_{14}O_{20}$	$[2M^{18}+H]^+$	1175.5904	1175.5903	−0.1
	$C_{47}H_{71}N_{15}O_{16}$	$[(M^{10}+M^{18})+H]^+$	1102.5238	1102.5276	3.4
(**7**, **9**, and **10**/**18**)	$C_{45}H_{65}N_{13}O_{18}$	$[(M^{7}+M^{18})+H]^+$	1076.4681	1076.4643	−3.5
	$C_{47}H_{69}N_{13}O_{20}$	$[(M^{9}+M^{18})+H]^+$	1136.4855	1136.4900	−4.0
	$C_{47}H_{71}N_{15}O_{16}$	$[(M^{10}+M^{18})+H]^+$	1102.5310	1102.5276	−3.1
	$C_{48}H_{82}N_{14}O_{20}$	$[2M^{18}+H]^+$	1175.5908	1175.5903	−0.5
	$C_{70}H_{99}N_{21}O_{26}$	$[(M^{9}+M^{10}+M^{18})+H]^+$	1650.7193	1650.7143	3.1
	$C_{70}H_{97}N_{19}O_{30}$	$[(2M^{9}+M^{18})+H]^+$	1684.6791	1684.6721	−4.1

[a] ESI-TOF/MS were recorded in the positive ion mode.

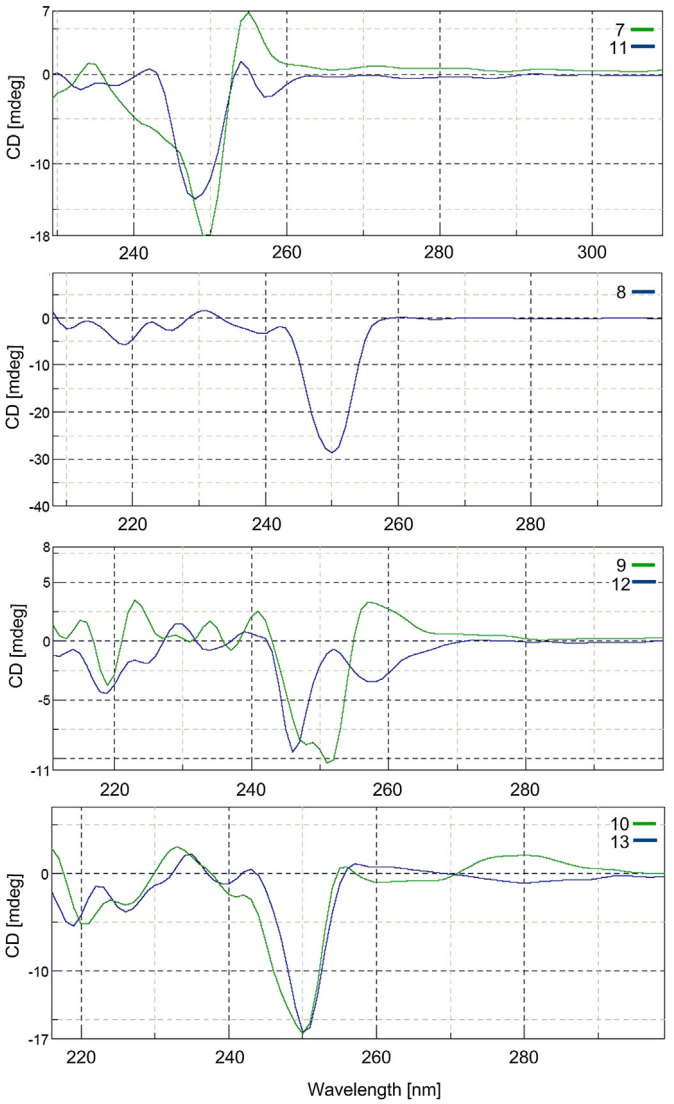

Fig. 12. CD spectra of the chiral receptors (**7**–**13**), samples were measured in DMSO.

obtained. Whenever possible the reactions were monitored by thin layer chromatography (TLC). TLC was performed on Macherey–Nagel aluminum backed plates pre-coated with silica gel 60 (UV_{254}). Melting points were determined in open capillaries using a Buechl B-545 melting point apparatus and are not corrected. Infrared spectra were determined using a Vector-33 Bruker FTIR spectrometer. The samples were measured directly as solids or oils; ν_{max} values were expressed in cm^{-1} and were given for the main absorption bands. ^1H NMR, ^{13}C NMR, and 2D ROESY spectra were acquired on a JEOL ECX-400 spectrometer operating at 400 MHz for ^1H NMR and 100 MHz for ^{13}C NMR in DMSO-d_6 using a 5 mm probe. The chemical shifts (δ) are reported in parts per million (ppm) and were referenced to the residual solvent peak. The following abbreviations are used: s, singlet; m, multiplet; br, broad signal. Mass spectra were recorded using HCTultra and ESI-TOF Bruker Daltonics mass spectrometers and samples were dissolved in DMF, CH_3CN, and H_2O using the ESI/+MS and ESI/−MS modes. Calibration was carried out using a 0.1 M solution of sodium formate in the enhanced quadratic mode prior to each experimental run. The results of measurements were processed using Compass 1.3 data analysis software for a Bruker Daltonics time-of-flight mass spectrometer (micrOTOF). Molecular modeling calculations were carried out with HyperChem software (Release 8.0.6) at the AM1 and PM3 levels in vacuo and no influence of solvents was taken into account in these calculations.[13]

Circular dichroism measurements were carried out using Jasco-J-810 Spectropolarimeter in H_2O and DMSO. Pre-loaded Wang resin, DIEA (*N*,*N*-diisopropylethylamine), HOBt [*O*-(benzotriazol-1-yl)-hydroxybenzotriazole], HBTU (*N*,*N*,*N*′,*N*′-tetramethyluranium hexafluorophosphate), 1-Fmoc (9-fluorenylmethoxycarbonyl)amino acid derivatives, DMF, NMP (*N*-methylpyrrolidone), TFA (trifluoroacetic acid), EDT (1,2-ethanedithiol) and other chemicals required for peptide synthesis were bought from Iris Biotech GmbH (Marktredwitz, Germany). Peptides were synthesized with a standard solid phase peptide synthesis technique and it was carried out on an automated peptide synthesizer (ABI-433A, Applied Biosystems, Foster City, USA). Fmoc protected pre-loaded resin was used to grow peptide chain on it. In detail, deprotection of the *N*-terminal of the resin bound amino acid was performed by 20% piperidine in NMP and the *C*-terminal of other protected amino acid was activated using HBTU/HOBt/DIEA (1:1:2) in DMF for coupling with the free *N*-terminal of the resin bound amino acid. A mixture of 82.5% TFA, 5% phenol, 5% H_2O, 5% thioanisole, and 2.5% EDT was used to separate the peptide from resin as well as to remove the side chain protecting groups. Subsequently, the peptide was isolated through precipitation in cold (−20 °C) Et_2O and lyophilized by Christ freeze dryers (Martin Christ Gefriertrocknungsanlagen GmbH, Osterode am Harz, Germany). Peptides were purified by HPLC (high performance liquid chromatography) and analyzed by HRMS. The dicarbohydrazides (**1**–**3**) were synthesized according to the Literature.[9a,b]

4.2. General procedure for preparation of chiral receptors (7–13)

To a stirred solution of the corresponding aryl isocyanates (**4**–**6**) (2 mmol) in anhydrous THF (6 mL) were added dicarbohydrazides (**1**–**3**) (1.1 mmol) in anhydrous THF (6 mL). The mixture was stirred at room temperature for 24 h. The solid was filtered, washed successively with H_2O, Et_2O, and dried to give the chiral dioxolane receptors (**7**–**13**).

*4.2.1. 2,2′-((4R,5R)-1,3-Dioxolane-4,5-dicarbonyl)bis(N-(4-methoxyphenyl)hydrazinecarboxamide) (**7**).* Prepared from (4*R*,5*R*)-1,3-dioxolane-4,5-dicarbohydrazide (**1**) and 4-methoxyphenyl isocyanate (**4**) (740 mg, 78%) as a white solid precipitate (mp 227–228); ν_{max} (solid) 3271, 1689 cm^{-1}; δ (400 MHz, DMSO-d_6) 10.05 (2H, br s, NHCO), 8.54 (2H, br s, NHCO), 8.04 (2H, br s, NHCO), 7.31 (4H, m, Ar*H*), 6.79 (4H, m, Ar*H*), 5.14 (2H, br s, OCH_2), 4.65 (2H, br s, CHCO), 3.65 (6H, br s, OMe) ppm; δ (100 MHz, DMSO-d_6) 169.3, 155.7, 155.0, 133.0, 120.8, 114.3, 97.0, 77.2, 55.6 ppm; *m*/*z* 487.0 (40, MH^-), 337.8 (100%); HRMS: MH^-, found 487.1588. $C_{21}H_{24}N_6O_8$ requires 487.1583.

*4.2.2. 2,2′-((2R,3R)-1,4-Dioxaspiro[4.5]decane-2,3-dicarbonyl)bis-(N-(4-methoxyphenyl)hydrazinecarboxamide) (**8**).* Prepared from (2*R*,3*R*)-1,4-dioxaspiro[4.5]decane-2,3-dicarbohydrazide (**2**) and 4-methoxyphenyl isocyanate (**4**) (800 mg, 74%). After 24 h of stirring at room temperature, H_2O was added and the solid was filtered as a white solid precipitate (mp>140 °C); ν_{max} (solid) 3294, 1681 cm^{-1}; δ (400 MHz, DMSO-d_6) 9.99 (2H, br s, NHCO), 8.51 (2H, br s, NHCO), 8.09 (2H, br s, NHCO), 7.32 (4H, m, Ar*H*), 6.76 (4H, m, Ar*H*), 4.63 (2H, br s, CHCO), 3.64 (6H, br s, OMe), 1.73–1.55 (6H, m, CH_2), 1.53–1.49 (2H, m, CH_2), 1.33 (2H, m, CH_2) ppm; δ (100 MHz, DMSO-d_6) 169.6, 156.1, 155.1, 132.8, 121.0, 114.4, 113.4, 76.8, 55.5, 36.0, 25.5, 25.2, 24.1 ppm; *m*/*z* 555.0 (52, MH^-), 405.9 (100%); HRMS: MH^-, found 555.2224. $C_{26}H_{32}N_6O_8$ requires 555.2209.

*4.2.3. 2,2′-((4R,5R)-1,3-Dioxolane-4,5-dicarbonyl)bis(N-(2,4-dimethoxyphenyl)hydrazinecarboxamide) (**9**).* Prepared from (4*R*,5*R*)-1,3-dioxolane-4,5-dicarbohydrazide (**1**) and 2,4-dimethoxyphenyl isocyanate (**5**) (711 mg, 93%) as a white solid precipitate (mp>190 °C); ν_{max} (solid) 3299, 1685 cm^{-1}; δ (400 MHz, DMSO-d_6) 10.11 (2H, br s, NHCO), 8.48 (2H, br s, NHCO), 7.88 (2H, br s, NHCO), 7.79 (2H, m, Ar*H*), 6.56 (2H, s, Ar*H*), 6.42 (2H, m, Ar*H*), 5.16 (2H, br s, OCH_2),

4.63 (2H, br s, CHCO), 3.79 (6H, br s, OMe), 3.68 (6H, br s, OMe) ppm; δ (100 MHz, DMSO-d_6) 169.1, 155.6, 155.4, 149.7, 122.0, 120.1, 104.6, 99.2, 97.0, 77.1, 56.3, 55.7 ppm; *m/z* 547.0 (66, MH^-), 367.9 (100%); HRMS: MH^-, found 547.1782. $C_{23}H_{28}N_6O_{10}$ requires 547.1794.

*4.2.4. 2,2′-((4R,5R)-1,3-Dioxolane-4,5-dicarbonyl)bis(N-(4-(dimethylamino)phenyl)hydrazinecarboxamide) (**10**).* Prepared from (4*R*,5*R*)-1,3-dioxolane-4,5-dicarbohydrazide (**1**) and 4-dimethylaminophenyl isocyanate (**6**) (705 mg, 89%) as a violet solid precipitate (mp>200 °C); ν_{max} (solid) 3263, 1688 cm^{-1}; δ (400 MHz, DMSO-d_6) 10.04 (2H, br s, NHCO), 8.37 (2H, br s, NHCO), 7.95 (2H, br s, NHCO), 7.21 (4H, d, *J* 9.1 Hz, Ar*H*), 6.62 (4H, d, *J* 9.1 Hz, Ar*H*), 5.14 (2H, br s, OCH_2), 4.65 (2H, br s, CHCO), 2.77 (12H, br s, NMe) ppm; δ (100 MHz, DMSO-d_6) 169.2, 155.8, 147.0, 129.7, 121.0, 113.5, 97.0, 77.2, 41.2 ppm; *m/z* 513.0 (70, MH^-), 350.9 (100%); HRMS: MH^-, found 513.2240. $C_{23}H_{30}N_8O_6$ requires 513.2216.

*4.2.5. 2,2′-((4S,5S)-1,3-Dioxolane-4,5-dicarbonyl)bis(N-(4-methoxyphenyl)hydrazinecarboxamide) (**11**).* Prepared from (4*S*,5*S*)-1,3-dioxolane-4,5-dicarbohydrazide (**3**) and 4-methoxyphenyl isocyanate (**4**) (910 mg, 96%) as a pale yellow solid precipitate (mp 224–225 °C); ν_{max} (solid) 3260, 1681 cm^{-1}; δ (400 MHz, DMSO-d_6) 10.05 (2H, br s, NHCO), 8.54 (2H, br s, NHCO), 8.04 (2H, br s, NHCO), 7.31 (4H, d, *J* 9.1 Hz, Ar*H*), 6.79 (4H, d, *J* 9.1 Hz, Ar*H*), 5.15 (2H, br s, OCH_2), 4.66 (2H, br s, CHCO), 3.65 (6H, br s, OMe) ppm; δ (100 MHz, DMSO-d_6) 169.3, 155.7, 155.0, 133.0, 120.9, 114.3, 97.0, 77.2, 55.6 ppm; *m/z* 486.9 (100, MH^-), 337.9 (19%); HRMS: MH^-, found 487.1570. $C_{21}H_{24}N_6O_8$ requires 487.1583.

*4.2.6. 2,2′-((4S,5S)-1,3-Dioxolane-4,5-dicarbonyl)bis(N-(2,4-dimethoxyphenyl)hydrazinecarboxamide) (**12**).* Prepared from (4*S*,5*S*)-1,3-dioxolane-4,5-dicarbohydrazide (**3**) and 2,4-dimethoxyphenyl isocyanate (**5**) (735 mg, 99%) as a pale yellow solid precipitate (mp>190 °C); ν_{max} (solid) 3297, 1696 cm^{-1}; δ (400 MHz, DMSO-d_6) 10.13 (2H, br s, NHCO), 8.50 (2H, br s, NHCO), 7.90 (2H, br s, NHCO), 7.90 (2H, m, Ar*H*), 6.57 (2H, s, Ar*H*), 6.42 (2H, m, Ar*H*), 5.18 (2H, br s, OCH_2), 4.66 (2H, br s, CHCO), 3.79 (6H, br s, OMe), 3.68 (6H, br s, OMe) ppm; δ (100 MHz, DMSO-d_6) 169.2, 155.6, 155.4, 149.7, 121.9, 120.2, 104.6, 99.2, 97.1, 77.2, 56.2, 55.7 ppm; *m/z* 547.0 (39, MH^-), 367.9 (100%); HRMS: MH^-, found 547.1799. $C_{23}H_{28}N_6O_{10}$ requires 547.1794.

*4.2.7. 2,2′-((4S,5S)-1,3-Dioxolane-4,5-dicarbonyl)bis(N-(4-(dimethylamino)phenyl)hydrazinecarboxamide) (**13**).* Prepared from (4*S*,5*S*)-1,3-dioxolane-4,5-dicarbohydrazide (**3**) and 4-dimethylaminophenyl isocyanate (**6**) (740 mg, 93%) as a violet solid precipitate (mp>210 °C); ν_{max} (solid) 3256, 1688 cm^{-1}; δ (400 MHz, DMSO-d_6) 10.04 (2H, br s, NHCO), 8.37 (2H, br s, NHCO), 7.95 (2H, br s, NHCO), 7.21 (4H, d, *J* 9.1 Hz, Ar*H*), 6.61 (4H, d, *J* 9.1 Hz, Ar*H*), 5.14 (2H, br s, OCH_2), 4.64 (2H, br s, CHCO), 2.76 (12H, br s, NMe) ppm; δ (100 MHz, DMSO-d_6) 169.3, 155.8, 147.0, 129.7, 121.0, 113.5, 97.0, 77.2, 41.2 ppm; *m/z* 513.1 (31, MH^-), 350.9 (100%); HRMS: MH^-, found 513.2233. $C_{23}H_{30}N_8O_6$ requires 513.2216.

Acknowledgements

H.N. thanks Deutscher Akademischer Austausch Dienst (DAAD) for financial support and Jacobs University for excellent facilities.

Supplementary data

^{1}H NMR, ^{13}C NMR, ESI-TOF/MS, MS/MS, proposed fragmentation mechanisms, and assembled structures of the new receptors with the carboxylic guests and oligopeptides. Supplementary data associated with this article can be found in the online version, at http://dx.doi.org/10.1016/j.tet.2013.11.002. These data include MOL file and InChiKey of the most important compound described in this article.

References and notes

1. (a) Otto, S. *Nat. Nanotechnol.* **2009**, *4*, 13; (b) Lee, I. *Langmuir* **2013**, *29*, 2476; (c) Palmer, L. C.; Stupp, S. I. *Acc. Chem. Res.* **2008**, *41*, 1674; (d) Hess, H.; Clemmens, J.; Brunner, C.; Doot, R.; Luna, S.; Ernst, K.-H.; Vogel, V. *Nano Lett.* **2005**, *5*, 629; (e) Zhang, S. *Nat. Nanotechnol.* **2006**, *1*, 169; (f) Seto, C. T.; Mathias, J. P.; Whitesides, G. M. *J. Am. Chem. Soc.* **1993**, *115*, 1321.
2. (a) Zhang, S. *Biotechnol. Adv.* **2002**, *20*, 321; (b) Zhang, S. *Nat. Biotechnol.* **2003**, *21*, 1171; (c) Reches, M.; Gazit, E. *Curr. Nanosci.* **2006**, *2*, 105; (d) Whitesides, G. M.; Mathias, J. P.; Seto, C. T. *Science* **1991**, *254*, 1312; (e) Gazit, E. *Nat. Nanotechnol.* **2008**, *3*, 8; (f) Weiß, T.; Schierbaum, K. D.; Thoden van Velzen, U.; Reinhoudt, D. N.; Göpel, W. *Sens. Actuators, B* **1995**, *26-27*, 203.
3. Beijer, F. H.; Kooijman, H.; Spek, A. L.; Sijbesma, R. P.; Meijer, E. W. *Angew. Chem., Int. Ed.* **1998**, *37*, 75.
4. Lee, H.-Y.; Olasz, A.; Pink, M.; Park, H.; Lee, D. *Chem. Commun.* **2011**, 481.
5. Ariga, K.; Hill, J. P.; Lee, M. V.; Vinu, A.; Charvet, R.; Acharya, S. *Sci. Technol. Adv. Mater.* **2008**, *9*, 014109.
6. (a) Caspar, D. L. D.; Namba, K. *Adv. Biophys.* **1990**, *26*, 157; (b) Klug, A. *Philos. Trans. R. Soc., B* **1999**, *354*, 531; (c) Butler, P. J. *Philos. Trans. R. Soc., B* **1999**, *354*, 537.
7. Hartgerink, J. D.; Beniash, E.; Stupp, S. I. *Science* **2001**, *294*, 1684.
8. (a) Engeser, M.; Rang, A.; Ferrer, M.; Gutiérrez, A.; Tarik Baytekin, T.; Schalley, C. A. *Int. J. Mass Spectrom.* **2006**, *255–256*, 185; (b) Schalley, C. A. *Int. J. Mass Spectrom.* **2000**, *194*, 11; (c) Schalley, C. A.; Castellano, R. K.; Brody, M. S.; Rudkevich, D. M.; Siuzdak, G.; Rebek, J., Jr. *J. Am. Chem. Soc.* **1999**, *121*, 4568; (d) Schalley, C. A.; Müller, T.; Linnartz, P.; Witt, M.; Schäfer, M.; Lützen, A. *Chem.—Eur. J.* **2002**, *8*, 3538; (e) Sherman, C. L.; Brodbelt, J. S.; Marchand, A. P.; Poola, B. *J. Am. Soc. Mass Spectrom.* **2005**, *16*, 1162; (f) Cziferszky, M.; Biedermann, F.; Kalberer, M.; Scherman, O. A. *Org. Biomol. Chem.* **2012**, *10*, 2447; (g) Ma, X.; Wei, Z.; Xiong, X.; Jiang, Y.; He, J.; Zhang, S.; Fang, X.; Zhang, X. *Talanta* **2012**, *93*, 252.
9. (a) Nour, H. F.; Hourani, N.; Kuhnert, N. *Org. Biomol. Chem.* **2012**, *10*, 4381; (b) Nour, H. F. *The Development of Novel Antibiotics Using Chemical Evolution* Thesis; Jacobs University: Bremen, 2012; (c) Nour, H. F.; Golon, A.; Kuhnert, N. *Tetrahedron Lett.* **2013**, *54*, 4139.
10. Skowronek, P.; Kuncewicz, M.; Brzostowska, M.; Janiak, A.; Rychlewska, U.; Gawroński, J. *Tetrahedron: Asymmetry* **2012**, *23*, 300.
11. Nour, H. F.; Islam, T.; Fernández-Lahore, M.; Kuhnert, N. *Rapid Commun. Mass Spectrom.* **2012**, *26*, 2865.
12. (a) Gawroński, J.; Kołbon, H.; Kwit, M.; Katrusiak, A. *J. Org. Chem.* **2000**, *65*, 5768; (b) Kuhnert, N.; Rossignolo, G. M.; López-Periago, A. M. *Org. Biomol. Chem.* **2003**, *1*, 1157; (c) Kuhnert, N.; Patel, C.; Jami, F. *Tetrahedron Lett.* **2005**, *46*, 7575; (d) Kuhnert, N.; López-Periago, A. M. *Tetrahedron Lett.* **2002**, *43*, 3329; (e) Kuhnert, N.; López-Periago, A. M.; Rossignolo, G. M. *Org. Biomol. Chem.* **2005**, *3*, 524; (f) Kuhnert, N.; Straßnig, C.; López-Periago, A. M. *Tetrahedron: Asymmetry* **2002**, *13*, 123; (g) Kuhnert, N.; Tang, B. *Tetrahedron Lett.* **2006**, *47*, 2985; (h) Kuhnert, N.; Marsh, D.; Nicolau, D. C. *Tetrahedron: Asymmetry* **2007**, *18*, 1648; (i) Nour, H. F.; Matei, M. F.; Bassil, B. S.; Kortz, U.; Kuhnert, N. *Org. Biomol. Chem.* **2011**, *9*, 3258.
13. (a) Molecular Modeling Was Carried Out Using HyperChem Software (Release 8.0.6). Hypercube: 1115 NW 4th Street, Gainesville, F1orida 32601 USA. Trial version from http://www.hypercube.com, 1995–2008. (b) Stewart, J. J. P. *J. Comput. Chem.* **1989**, *10*, 221.
14. (a) Alfonso, I.; Bolte, M.; Bru, M.; Burguete, M. I.; Luis, S. V.; Vicent, C. *Org. Biomol. Chem.* **2010**, *8*, 1329; (b) Schug, K.; Fryčák, P.; Maier, N. M.; Lindner, W. *Anal. Chem.* **2005**, *77*, 3660; (c) Arakawa, R.; Kobayashi, M.; Fukuo, T.; Shiraiwa, T. *Rapid Commun. Mass Spectrom.* **2001**, *15*, 685.
15. Nour, H. F.; López-Periago, A. M.; Kuhnert, N. *Rapid Commun. Mass Spectrom.* **2012**, *26*, 1070.
16. Nour, H. F.; Golon, A.; Kuhnert, N. Unpublished results.